JACS
JOURNAL OF THE AMERICAN CHEMICAL SOCIETY
Article
pubs.acs.org/JACS

Exceptional Chemical Properties of Sc@C_{2v}(9)–C_{82} Probed with Adamantylidene Carbene

Makoto Hachiya,[†] Hidefumi Nikawa,[†] Naomi Mizorogi,[†] Takahiro Tsuchiya,[†] Xing Lu,*[,†,‡] and Takeshi Akasaka*[,†]

[†]Life Science Center of Tsukuba Advanced Research Alliance, University of Tsukuba, Ibaraki 305-8577, Japan

[‡]State Key Laboratory of Materials Processing and Die & Mold Technology, College of Materials Science and Engineering, Huazhong University of Science and Technology (HUST), 1037 Luoyu Road, Wuhan 430074, China

Supporting Information

ABSTRACT: It has been an interesting finding that reactions of M@C_{2v}(9)–C_{82} (M = Y, La, Ce, Gd) with diazirine adamantylidene (AdN_2, **1**) gave rise to only two monoadduct isomers, indicating that the cage reactivity of monometallofullerenes is not dependent on the type of the internal metal. However, we found here that Sc@C_{2v}(9)–C_{82} shows an exceptional chemical reactivity toward the electrophile **1**, affording four monoadduct isomers (**2a–d**). Single-crystal X-ray diffraction crystallographic results of the most abundant isomer (**2a**) confirm that the addition takes place at a [6,6]-bond junction which is very close to the internal metal ion. Theoretical calculations reveal that 2 out of the 24 nonequivalent cage carbons of Sc@C_{2v}(9)–C_{82} are highly reactive toward **1**, but only one cage carbon of the other M@C_{2v}–C_{82} (M = Y, La, Ce, Gd) is sufficiently reactive. The exceptional chemical property of Sc@C_{2v}(9)–C_{82} is associated with the small ionic radius of Sc^{3+}, which allows stronger metal–cage interactions and makes back-donation of charge from the cage to the metal more pronounced. Our results have provided new insights into the art of altering the chemical properties of fullerene molecules at the atomic level, which would be useful in the future in utilizing EMFs in quantum computing systems.

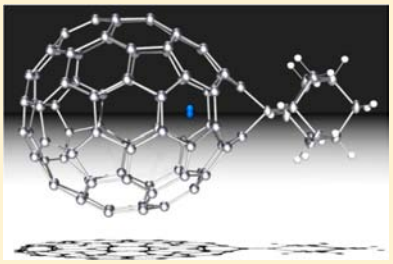

INTRODUCTION

The hollow cavities of fullerenes can host a variety of metal atoms and even metallic clusters, thus generating a new family of spherical molecules with unique structures, novel properties, and potential applications in biomedicine, electronics, photovoltaics, and materials sciences.[1] This new class of hybrid materials is now commonly called endohedral metallofullerenes (EMFs). During the past two decades, extensive efforts have been devoted to putting different kinds of metallic complexes inside fullerenes. It was found that one metal or two metal atoms can be simply incarcerated inside fullerenes, but three or more metal atoms tend to form metallic clusters with nonmetallic elements, forming cluster EMFs of many kinds.[2] Strong interactions between the encaged metallic species and the fullerene cage were observed, which makes EMFs more complicated and more fascinating than empty fullerenes, and accordingly they are expected to be more useful.

In recent years, with progress achieved in the synthesis and isolation processes of EMFs, macroscopic amounts of some typical EMF isomers have become readily available. Taking advantage of this, chemical modifications of EMFs have become a hot topic. Various kinds of derivatives of EMFs have been synthesized and characterized.[3−6] Besides the achievements in successful generation of several applicable materials based on EMFs,[7] of fundamental importance is the finding that encapsulated metal species strongly affect the chemical properties of the whole molecule. Different chemical reactivities of EMFs dictated by the internal metallic species were first observed between a cluster metallofullerene Sc_3N@C_{80} and a dimetallofullerene La_2@C_{80}, both having the same I_h–C_{80} cage structure and the same electronic configuration described as M^{6+}@C_{80}^{6-}.[8] When probed with a disilirane reagent, La_2@C_{80} showed both thermal and photochemical reactivities but Sc_3N@C_{80} reacted only photochemically.[8] Different chemical behaviors were also found among EMFs containing a trimetallic nitride cluster, the so-called TNT family.[2,4,6] For instance, Y_3N@C_{80} undergoes Bingel reaction and Prato reaction easily, affording exclusively [6,6]-adducts, but Sc_3N@C_{80} does not undergo Bingel reaction, and its Prato derivatives are [5,6]-adducts.[4,6,9] These differences are interpreted by the strong interactions between the encapsulated metallic clusters and the fullerene cage: the larger Y_3N cluster makes the I_h–C_{80} cage more reactive.[9] Nevertheless, since cluster fullerenes have a more crowded core than mono-EMFs, as evidenced from the shorter metal–cage distances,[10] it seems not so surprising that the encaged nitride cluster strongly affects the cage shell in terms of chemical properties.

For mono-EMFs, M@C_{82}-type species (M = trivalent rare earth elements) have received more attention than others because of their relatively high production yields. It was revealed both theoretically and experimentally that the trivalent metal ion in M@C_{2v}–C_{82} (M = Y, La, Ce, and Gd) is not localized in the center of the cage but is positioned closely

Received: July 15, 2012
Published: August 22, 2012

   dx.doi.org/10.1021/ja306890x | J. Am. Chem. Soc. 2012, 134, 15550–15555

under a hexagonal ring along the C_2 axis.[11] This off-center location of the encaged metal ion makes the adjacent carbons highly pyramidalized and engenders the electron density distribution highly anisotropic over the cage surface.[12] As a result, a cage carbon closest to the metal is far more reactive than others toward the electrophile diazirine adamantylidene (AdN_2, **1**), thus affording only two monoadduct isomers, although there are 24 nonequivalent carbons on the $C_{2v}(9)$–C_{82} cage. Interestingly, even when a different metal atom (Y, La, Ce, or Gd) is encapsulated inside the $C_{2v}(9)$–C_{82} cage, the whole molecule showed identical reactivity toward the electrophile **1**.[13] Thus, it appears that a single metal ion in mono-EMFs does not affect the reactivity of cage carbons evidently.

In this article, we report our recent findings related to the exceptional chemical reactivity of Sc@C_{82} probed with **1**. Distinctly different from the results obtained from reactions between **1** and other M@$C_{2v}(9)$–C_{82} (M = Y, La, Ce, and Gd) which gave rise to only two monoadduct isomers,[13] reaction of Sc@$C_{2v}(9)$–C_{82} with **1** affords four monoadduct isomers (**2a**–**d**) which were fully characterized with various experimental techniques. The molecular structure of the most abundant isomer (**2a**) was unambiguously determined by the single-crystal X-ray diffraction method. With the assistance of theoretical calculations, we found that two cage carbons of Sc@$C_{2v}(9)$–C_{82} are sufficiently reactive toward the electrophile **1**. Such a strong metal–cage interaction results from the small ionic radius of Sc^{3+}, which ensures its close contact with the cage and makes the back-donation of electrons from the negatively charged cage to the metal highly efficient. This presents the first example for EMFs that one single metal ion can affect the properties of the whole molecule so markedly.

EXPERIMENTAL SECTION

In a typical synthesis, a degassed toluene solution (10 mL) containing both Sc@C_{82} (MW 1029, 1.0 mg, 9.72×10^{-5} M) and 2-adamantane-2,3-[3*H*]-diazirine (**1**, $C_{10}H_{14}N_2$, MW 162, 2.0 mg, 1.23×10^{-3} M) in a sealed tube was irradiated with an ultra-high-pressure mercury arc lamp (cutoff < 350 nm) at room temperature (Scheme 1).[13] The

Scheme 1. Photoreaction of Sc@C_{82} with 1

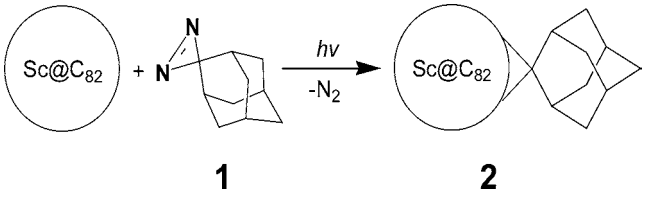

reaction was monitored with high-performance liquid chromatography (HPLC). Figure 1 shows the HPLC profiles monitored at different reaction times. Before irradiation, **1** and Sc@C_{82} had two peaks at 4 and 30 min, respectively. After being irradiated for 2 s, new peaks appeared between 11 and 15 min, which are monoadduct isomers, as confirmed by mass spectrometry. By prolonging the irradiation time, the content of monoadducts increased rapidly. In order to get monoadducts only, the reaction was terminated after the mixture was irradiated for 12 s when a small amount of multiadducts was generated. Subsequent HPLC separations with a Buckyprep column gave four monoadduct isomers, i.e., **2a**, **2b**, **2c**, and **2d** with relative abundances of 40%, 25%, 25%, and 10%, respectively.

Preparative high-performance liquid chromatography (HPLC) was conducted on an LC-908 machine (Japan Analytical Industry Co., Ltd.) with toluene as the mobile phase. Matrix-assisted laser desorption/ionization time-of-flight (MALDI-TOF) mass spectrometry was performed on a BIFLEX III machine (Bruker, Germany) with 1,1,4,4-tetraphenyl-1,3-butadiene (TPB) as the matrix. UV–vis–NIR spectra were measured on a UV 3150 spectrometer (Shimadzu, Japan) in CS_2. NMR spectra were obtained with a Bruker AVANCE-500 spectrometer in CS_2/acetone-d_6 (v:v = 1:1). Cyclic voltammetry (CV), differential pulse voltammetry (DPV), and bulk electrolysis were performed in 1,2-dichlorobenzene with 0.1 M $(n\text{-Bu})_4NPF_6$ with Pt as the working electrode on a potentiostat/galvanostat workstation (BAS CW-50). The scan rate of CV was 20 mV s^{-1}. Conditions of DPV: pulse amplitude, 50 mV; scan rate, 20 mV s^{-1}. The potential was set to be constant at −500 mV relative to the saturated calomel electrode (SCE) in the bulk electrolysis experiment of **2a**. XRD measurement was performed on a Bruker APEX II machine equipped with a CCD camera. The structure was solved with direct methods and refined using SHLEX 97.[14]

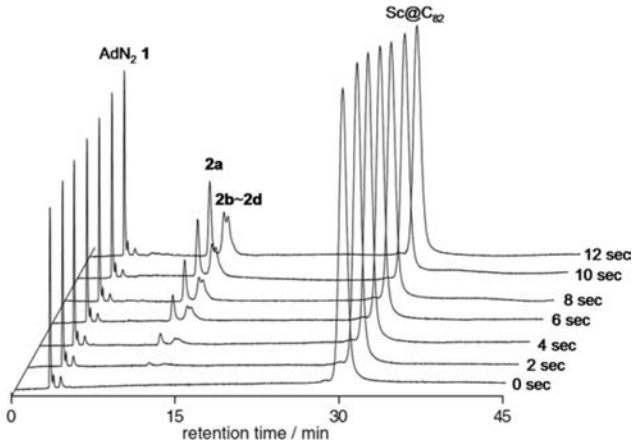

Figure 1. HPLC profiles of the reaction mixture of Sc@$C_{2v}(9)$–C_{82} and **1**. Conditions: Buckyprep column (Nakalai Tesque), 1.0 mL/min toluene flow, 330 nm detection wavelength, 40 °C.

Theoretical calculations were carried out using the Gaussian 03 program package.[15] Molecular structures were optimized at the B3LYP/3-21G(d)[16] level with the B3LYP density functional.[17]

Black crystals of **2a** were obtained by layering a CS_2 solution at the bottom of hexane in a glass tube (φ = 7 mm). After a period of 2 weeks, black crystalline rods appeared at the bottom of the tube. A piece of crystal with dimensions of 0.30 mm × 0.10 mm × 0.10 mm was found suitable for XRD measurement and provided the corresponding structural information of **2a**.

RESULTS AND DISCUSSION

Formation of the monoadducts is confirmed firmly by mass spectrometry. The spectrum of **2a** is shown in Figure 2 as a representative, and all others are essentially identical. A single peak at m/z 1163 is readily observed, which is ascribed to Sc@$C_{82}(C_{10}H_{14})$, confirming formation of the 1:1 adduct. The absence of any fragmentation peak indicates the high stability of the adducts. The high stability of the corresponding Ad derivatives of EMFs ensures their superior application in such fields as photovoltaics.[13]

Electron spin resonance (ESR) spectrometry was first adopted to characterize the electronic structures of these monoadduct isomers. As shown in Figure 3, pristine Sc@$C_{2v}(9)$–C_{82} shows distinct hyperfine splitting octets at g = 2.0005 with a hyperfine coupling constant (hfcc) of 3.78 G. The four monoadducts (**2a**–**d**) also show distinct hyperfine octets with different hfcc values, confirming that the local environments of the metal nuclei in these four isomers are mutually different. The presence of the ESR patterns in **2a**–**d** confirms that all derivatives are cycloadducts.[13]

dx.doi.org/10.1021/ja306890x | J. Am. Chem. Soc. 2012, 134, 15550–15555

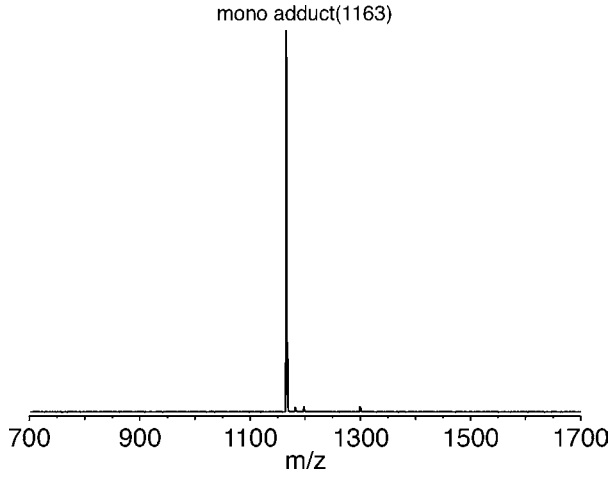

Figure 2. MALDI TOF spectrum of **2a** in a negative reflection mode.

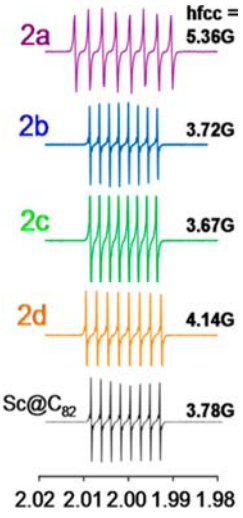

Figure 3. ESR spectra of Sc@$C_{2v}(9)$−C_{82}, **2a**−**d**.

The electronic properties of the derivatives were further investigated with vis−NIR spectrometry. As displayed in Figure 4, the spectrum of Sc@$C_{2v}(9)$−C_{82} shows two characteristic absorption peaks at 630 and 780 nm with two broad bands centered at 1100 and 1500 nm. The onset is observed at 1900 nm, consistent with a small optical band gap (~0.65 eV). Spectra of **2a**−**d** are similar to that of pristine Sc@$C_{2v}(9)$−C_{82} with slight alternations in the broad band region between 1000 and 1900 nm. These features indicate that the π system of Sc@$C_{2v}(9)$−C_{82} is not significantly altered by Ad addition, which implies that all monoadduct isomers have open structures, as previously found for the corresponding Ad adducts of other EMFs.[13]

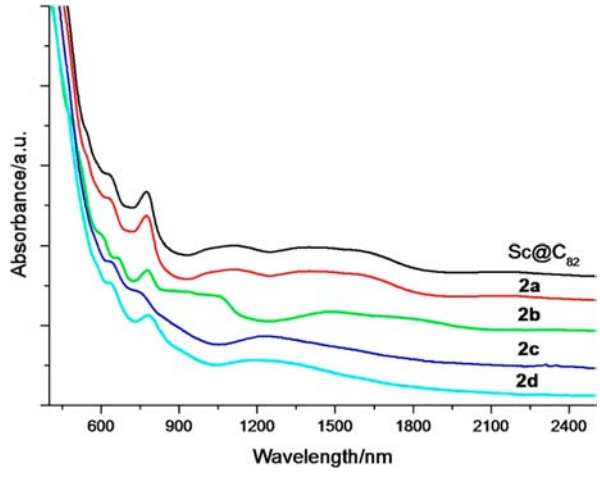

Figure 4. Vis−NIR spectra of Sc@$C_{2v}(9)$−C_{82}, **2a**−**d**.

The electrochemical behavior of **2a**−**d** is also similar to that of pristine Sc@$C_{2v}(9)$−C_{82}, but their redox potentials (Table 1)

Table 1. Redox Potentials (V vs Fc/Fc$^+$)[a] of Sc@C_{82}, 2a−d

compound	$^{ox}E_1$	$^{red}E_1$	$^{red}E_2$
Sc@C_{82}[b]	+0.15	−0.35	−1.29
2a	+0.09	−0.39	−1.43
2b	+0.09	−0.37	−1.39[b]
2c	+0.05	−0.42	−1.40[b]
2d	−0.04	−0.43	

[a]Half-cell potentials unless otherwise noted. [b]Irreversible DPV value.

are cathodically shifted as compared with the corresponding values of Sc@$C_{2v}(9)$−C_{82}, which again confirms the weak electron-donating ability of Ad to metallofullerenes.[13] Accordingly, it would be conclusive that the Ad cycloaddition reaction is a practical strategy to get more stable and more useful derivatives of EMFs in photovoltaics.

To obtain structural information on the derivatives, ^{13}C NMR spectroscopy was first performed on the most abundant isomer (**2a**). To do so the paramagnetic **2a** has to be reduced electrochemically, and the anion was then subjected to NMR characterization. The spectrum is shown in Figure S1, Supporting Information. In total, 82 signals were observed in the aromatic region, indicative of the C_1 symmetry of the whole molecule. The two peaks at 99.6 and 106.4 ppm can be assigned to the two cage carbons at the sites of addition, which confirms that **2a** has an open-cage structure.[13]

Good single crystals of **2a** suitable for XRD measurement were obtained by a diffusion method, and the molecular structure of **2a** was unambiguously established, as shown in Figure 5. The Ad moiety adds to one of the [6,6]-bonds closest to the internal metal. The distance between C1 and C2 is 2.107 Å, establishing the open-cage structure of **2a**. In spite of the difference of the internal metal, the structure of **2a** is essentially identical to those of M@$C_{2v}(9)$−C_{82}(Ad) (M = La,[13a] Gd,[13b]

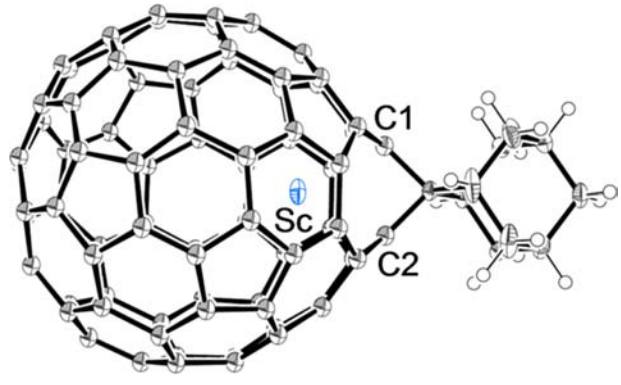

Figure 5. ORTEP drawing of an enantiomer of **2a** showing thermal ellipsoid at the 50% probability level. Solvent molecules are omitted for clarity.

dx.doi.org/10.1021/ja306890x | J. Am. Chem. Soc. 2012, 134, 15550−15555

Y^{13c}), proving that the Sc atom in pristine Sc@$C_{2v}(9)$−C_{82} is located under the hexagonal ring along the C_2 axis. Sc−C1 and Sc−C2 distances are 2.323 and 2.308 Å, respectively, which are shorter than the corresponding metal−carbon distances in other M@C_{82}(Ad) (M = Y, La, Gd) because of the smaller radius of Sc^{3+}.

Table 2 lists the interatomic distances between the incarcerated metal cation and the two cage carbons at the

Table 2. Ionic Radii of M^{3+} and Selected Interatomic Distances in M@$C_{2v}(9)$−C_{82}(Ad) (Angstroms)

M@C_{82}(Ad)	M^{3+} radius	M−C1	M−C2	C1−C2
M = Sc	0.745	2.323	2.308	2.107
M = Y	0.900	2.475	2.466	2.107
M = La	1.061	2.658	2.634	2.097
M = Gd	0.938	2.523	2.515	2.100

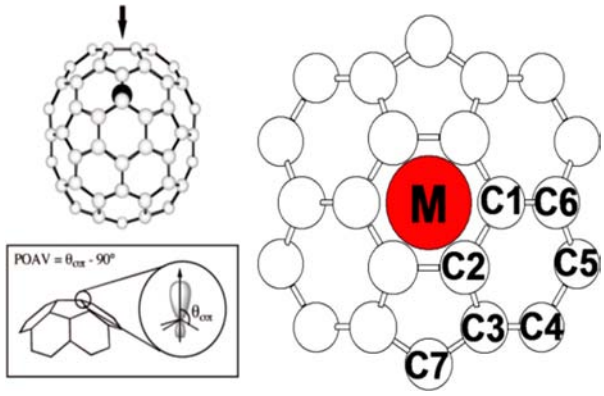

Figure 6. Schematic illustration of M@C_{2v}−C_{82}.

sites of addition, i.e., C1 and C2 as labeled in Figure 6, which are obtained from the X-ray results of M@$C_{2v}(9)$−C_{82}Ad (M = Sc, Y, La, Gd),[13] together with the ionic radii of M^{3+} to ease comprehension. The M−C1 and M−C2 distances increase consistently with increasing M^{3+} radii, but the C1−C2 distance remains nearly constant. These results indicate that the metal cation in pristine M@C_{82} (M = Sc, Y, La, Gd) interacts strongly with the adjacent carbons consisting of the hexagonal ring. The off-center position of the metal ion and its strong interaction with the cage brings anisotropic distributions of electron densities on the fullerene cage and thus differentiate the chemical properties of the cage carbons. For example, the electrophile AdN_2 (**1**) tends to attack the electron-rich carbon of La@$C_{2v}(9)$−C_{82}, which is close to the metal,[13a] while the carbanion prefers to react with the positively charged cage carbons distant from the metal.[12]

It has been demonstrated that the reactivity of cage carbons of fullerenes depends strongly on the local strain on each carbon atom. The pyramidalization angles from the p-orbital axis vector (POAV)[18] analyses provide a useful index of the local strain. However, we found that charge density values are more effective than POAV values for determining the reactivity of cage carbons of EMFs toward the electrophile **1**.[13] Thus, we calculated the charge density values of Sc@$C_{2v}(9)$−C_{82} to understand its exceptional chemical properties. Table 3 shows the related data of the carbon atoms labeled in Figure 6 together with the corresponding values of other M@$C_{2v}(9)$−C_{82} (M = Y, La, Gd) for comparison. It is obvious that the two types of carbon atoms (C1 and C2) consisting of the hexagonal ring which is very close to the metal ion in these endohedrals have much higher charge density values than others. When the encaged metal is Y, La, or Gd, only C1 is sufficiently reactive toward **1**, affording two monoadduct isomers. Thus, it may be deduced that a charge density value higher than −0.15 is necessary for a cage carbon of M@$C_{2v}(9)$−C_{82} to react with the electrophile **1**. In Sc@$C_{2v}(9)$−C_{82}, both C1 and C2 have charge density values higher than that of C1 in other M@C_{82} (M = Y, La, Gd). Accordingly, not only C1 but also C2 is sufficiently reactive to **1** in Sc@$C_{2v}(9)$−C_{82}. After being linked with C1 or C2, the Ad group then connects with an adjacent carbon to form the final adducts. Thus, in total four isomers are generated for Sc@$C_{2v}(9)$−C_{82}. **2a**, formed by addition of Ad to C1 and C2, has the highest yield because both C1 and C2 are sufficiently reactive with **1**. This is in perfect agreement with the experimental results. Schematic illustrations of the molecular structures of all four isomers (**2a**−**d**) are collectively shown in Figure S2, Supporting Information.

To fully understand the exceptional chemical property of Sc@$C_{2v}(9)$−C_{82}, theoretical calculations were performed. It is well known that electron transfer from the internal metal to the cage takes place in EMFs. In M@$C_{2v}(9)$−C_{82} (M = Sc, Y, La, Gd), three electrons are donated from the metal to the cage, and the electronic structure of M@$C_{2v}(9)$−C_{82} can be described as M^{3+}@C_{82}^{3-}. Consequently, an unpaired electron lies in the highest occupied molecular orbital (HOMO) of the molecule and brings paramagnetism to these EMFs. Previous results have discovered that back-donation of charges from the cage to the metal always occurs in EMFs. For example, the singly occupied molecule orbital (SOMO) of La@$C_{2v}(9)$−C_{82} contains 0.9% contribution from the d orbital of La (Figure 7a). Surprisingly, our calculations of Sc@$C_{2v}(9)$−C_{82} reveal that the back-donation of the negative charge from the cage to the Sc caion is much more pronounced than the situation in La@C_{82}. As shown in Figure 7b, the SOMO of Sc@$C_{2v}(9)$−C_{82} localizes not only on the carbon cage but also partially on the Sc cation. The contribution of the d orbital of Sc to the SOMO of Sc@$C_{2v}(9)$−C_{82} is up to 6.2%. Obviously, such an extra dative bonding between Sc^{3+} and the cage should account for the highly anisotropic distributions of charge densities on the Sc@$C_{2v}(9)$−C_{82} cage, and resultantly for the exceptional chemical reactivity of cage carbons. Such a stronger Sc−cage interaction should be originated from the smaller ionic radius of Sc^{3+},

Table 3. Charge Density Values (arbitrary units) of Selected Carbons of M@$C_{2v}(9)$−C_{82}

EMF	C1	C2	C3	C4	C5	C6
Sc@C_{82}	−0.215	−0.188	−0.089	−0.066	−0.014	−0.110
Y@C_{82}	−0.172	−0.135	−0.076	−0.071	−0.018	−0.096
La@C_{82}	−0.170	−0.136	−0.071	−0.092	−0.037	−0.099
Gd@C_{82}	−0.175	−0.123	−0.060	−0.058	−0.002	−0.086

dx.doi.org/10.1021/ja306890x | J. Am. Chem. Soc. 2012, 134, 15550−15555

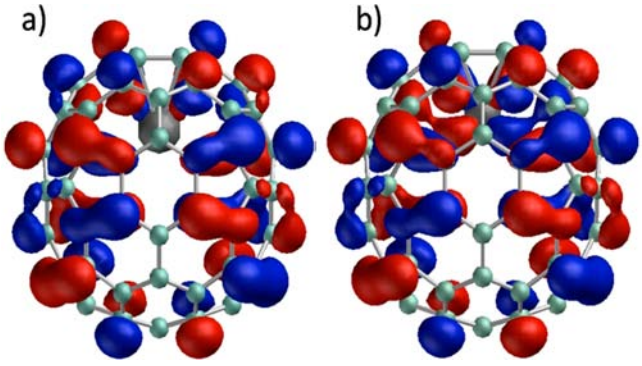

Figure 7. SOMO diagrams of (a) La@C_{2v}(9)−C_{82} and (b) Sc@C_{2v}(9)−C_{82}.

which allows a closer contact of the molecular orbitals between the metal cation and the nearby cage carbons.

CONCLUSION

Exceptional chemical properties were found for Sc@C_{2v}(9)−C_{82}, presenting the first example for EMFs in which a single metal ion jailed inside the fullerene cage can affect the chemical properties of the whole molecule markedly. Reaction of the carbene reagent **1** with Sc@C_{2v}(9)−C_{82} gave rise to four monoadduct isomers (**2a**−**d**), but only two isomers were obtained for the other M@C_{2v}(9)−C_{82} (M = Y, La, Ce, Gd) EMFs.[13] Single-crystallographic results of the most abundant isomer of Sc@C_{82}(Ad) confirm that the Ad group tends to attack the carbon atoms consisting of the hexagonal ring closest to the Sc atom. In combination with theoretical calculations, it was found that two carbons on the cage of Sc@C_{2v}(9)−C_{82} are sufficiently reactive toward **1**, but only one carbon is adequately reactive in other M@C_{82}-type EMFs (M = Y, La, Ce, Gd). The exceptional chemical property of Sc@C_{2v}(9)−C_{82} is tightly associated with the small radius of Sc^{3+}, which ensures the close metal−cage contact and makes the charge back-donation from the cage to the metal more efficient. Our results have enhanced our knowledge about the metal−cage interactions, molecular structures, and physicochemical properties of EMFs and will be informative to future works dealing with generation of applicable materials based on EMF derivatives.

ASSOCIATED CONTENT

Supporting Information

Complete author list of refs 7a, 13a, 13b, and 15, NMR spectra, schematic illustration of the structures of **2a**−**d**, and crystal data of Sc@C_{82}Ad (**2a**). This material is available free of charge via the Internet at http://pubs.acs.org.

AUTHOR INFORMATION

Corresponding Author

E-mail: lux@mail.hust.edu.cn; akasaka@tara.tsukuba.ac.jp

Notes

The authors declare no competing financial interest.

ACKNOWLEDGMENTS

Financial support from MEXT (No. 20108001 "pi-Space", No. 20245006), a Grand0in-Aid for Scientific Research (A) (No. 20245006) and (B) (No. 24350019) and The Strategic Japanese-Spanish Cooperative Program funded by JST and MICINN is gratefully acknowledged. XL appreciates the generous financial support from The National Thousand Talents Program, The National Natural Science Foundation of China (No. 21171061), and HUST.

REFERENCES

(1) (a) Akasaka, T.; Nagase, S. *Endofullerenes: A New Family of Carbon Clusters*; Kluwer: Dordrecht, The Netherlands, 2002. (b) Akasaka, T.; Wudl, F.; Nagase, S. *Chemisty of Nanocarbons*; John Wiley & Sons Ltd.: Chichester, 2010. (c) Lu, X.; Akasaka, T.; Nagase, S. In *Rare Earth Coordination Chemistry: Fundamentals and Applications*; Huang, C. H., Ed.; Wiley-Blackwell: Singapore, 2009; pp 273−308.

(2) (a) Dunsch, L.; Yang, S. *Small* **2007**, *3*, 1298−1320. (b) Chaur, M. N.; Melin, F.; Ortiz, A. L.; Echegoyen, L. *Angew. Chem., Int. Ed.* **2009**, *48*, 7514−7538. (c) Rodríguez-Fortea, A.; Balch, A. L.; Poblet, J. M. *Chem. Soc. Rev.* **2011**, *40*, 3551−3563. (d) Lu, X.; Akasaka, T.; Nagase, S. *Chem. Commun.* **2011**, *47*, 5942−5957. (e) Maeda, Y.; Tsuchiya, T.; Lu, X.; Takano, Y.; Akasaka, T.; Nagase, S. *Nanoscale* **2011**, *3*, 2421−2429. (f) Akasaka, T.; Lu, X. *The Chem. Rec.* **2012**, *12*, 256−269. (g) Lu, X.; Feng, L.; Akasaka, T.; Nagase, S. *Chem. Soc. Rev.* DOI:10.1039/c2cs35214a.

(3) (a) Akasaka, T.; Kato, T.; Kobayashi, K.; Nagase, S.; Yamamoto, K.; Funasaka, H.; Takahashi, T. *Nature* **1995**, *374*, 600−601. (b) Yamada, M.; Wakahara, T.; Nakahodo, T.; Tsuchiya, T.; Maeda, Y.; Akasaka, T.; Yoza, K.; Horn, E.; Mizorogi, N.; Nagase, S. *J. Am. Chem. Soc.* **2006**, *128*, 1402−1403. (c) Wakahara, T.; Iiduka, Y.; Ikenaga, O.; Nakahodo, T.; Sakuraba, A.; Tsuchiya, T.; Maeda, Y.; Kako, M.; Akasaka, T.; Yoza, K.; Horn, E.; Mizorogi, N.; Nagase, S. *J. Am. Chem. Soc.* **2006**, *128*, 9919−9925. (d) Wakahara, T.; Nikawa, H.; Kikuchi, T.; Nakahodo, T.; Rahman, G. M. A.; Tsuchiya, T.; Maeda, Y.; Akasaka, T.; Yoza, K.; Horn, E.; Yamamoto, K.; Mizorogi, N.; Slanina, Z.; Nagase, S. *J. Am. Chem. Soc.* **2006**, *128*, 14228−14229.

(4) (a) Iezzi, E. B.; Duchamp, J. C.; Harich, K.; Glass, T. E.; Lee, H. M.; Olmstead, M. M.; Balch, A. L.; Dorn, H. C. *J. Am. Chem. Soc.* **2002**, *124*, 524−525. (b) Cai, T.; Ge, Z.; Iezzi, E. B.; Glass, T. E.; Harich, K.; Gibson, H. W.; Dorn, H. C. *Chem. Commun.* **2005**, 3594−3596. (c) Shu, C.; Slebodnick, C.; Xu, L.; Champion, H.; Fuhrer, T.; Cai, T.; Reid, J.; Fu, W.; Harich, K.; Dorn, H. C.; Gibson, H. W. *J. Am. Chem. Soc.* **2008**, *130*, 17755−17760. (d) Wang, G.-W.; Liu, T.-X.; Jiao, M.; Wang, N.; Zhu, S.-E.; Chen, C.; Yang, S.; Bowles, F. L.; Beavers, C. M.; Olmstead, M. M.; Mercado, B. Q.; Balch, A. L. *Angew. Chem., Int. Ed.* **2011**, *50*, 4658−4662.

(5) (a) Lu, X.; He, X.; Feng, L.; Shi, Z.; Gu, Z. *Tetrahedron* **2004**, *60*, 3713−3716. (b) Lu, X.; Xu, J.; He, X.; Shi, Z.; Gu, Z. *Chem. Mater.* **2004**, *16*, 953−955. (c) Lu, X.; Zhou, X.; Shi, Z; Gu, Z. *Inorg. Chim. Acta* **2004**, *357*, 2397−2400. (d) Li, F.; Fan, L.; Liu, D.; Sung, H. H. Y.; Williams, I. D.; Yang, S.; Tan, K.; Lu, X. *J. Am. Chem. Soc.* **2007**, *129*, 10636−10637. (e) Lu, X.; Nikawa, H.; Tsuchiya, T.; Akasaka, T.; Toki, M.; Sawa, H.; Mizorogi, N.; Nagase, S. *Angew. Chem., Int. Ed.* **2010**, *49*, 594−597. (f) Lu, X.; Nakajima, K.; Iiduka, Y.; Nikawa, H.; Tsuchiya, T.; Mizorogi, N.; Slanina, Z.; Nagase, S.; Akasaka, T. *Angew. Chem., Int. Ed.* **2012**, *51*, 5889−5892.

(6) (a) Cardona, C. M.; Kitaygorodskiy, A.; Ortiz, A.; Herranz, M. A.; Echegoyen, L. *J. Org. Chem.* **2005**, *70*, 5092−5097. (b) Echegoyen, L.; Chancellor, C. J.; Cardona, C. M.; Elliott, B.; Rivera, J.; Olmstead, M. M.; Balch, A. L. *Chem. Commum.* **2006**, 2653−2655. (c) Lukoyanova, O.; Cardona, C. M.; Rivera, J.; Lugo-Morales, L. Z.; Chancellor, C. J.; Olmstead, M. M.; Rodriguez-Fortea, A.; Poblet, J. M.; Balch, A, L.; Echegoyen, L. *J. Am. Chem. Soc.* **2007**, *129*, 10423−10430.

(7) (a) Tsuchiya, T.; et al. *J. Am. Chem. Soc.* **2008**, *130*, 450−451. (b) Pinzon, J. R.; Plonska-Brzezinska, M. E.; Cardona, C. M.; Athans, A. J.; Gayathri, S. S.; Guldi, D. M.; Herranz, M. A.; Martin, N.; Torres, T.; Echegoyen, L. *Angew. Chem., Int. Ed.* **2008**, *47*, 4173−4176. (c) Bolskar, R. D. *Nanomedicine* **2008**, *3*, 201−213. (d) Ross, R. B.; Cardona, C. M.; Guldi, D. M.; Sankaranarayanan, S. G.; Reese, M. O.; Kopidakis, N.; Peet, J.; Walker, B.; Bazan, G. C.; Van Keuren, E.; Holloway, B. C.; Drees, M. *Nat. Mater.* **2009**, *8*, 208−212. (e) Ross, R. B.; Cardona, C. M.; Swain, F. B.; Guldi, D. M.; Sankaranarayanan, S.

G.; Van Keuren, E.; Holloway, B. C.; Drees, M. *Adv. Funct. Mater.* **2009**, *19*, 2332−2337.
(8) Iiduka, Y.; Ikenaga, O.; Sakuraba, A.; Wakahara, T.; Tsuchiya, T.; Maeda, Y.; Nakahodo, T.; Akasaka, T.; Kako, M.; Mizorogi, N.; Nagase, S. *J. Am. Chem. Soc.* **2005**, *127*, 9956−9957.
(9) Cardona, C. M.; Kitaygorodskiy, A.; Echegoyen, L. *J. Am. Chem. Soc.* **2005**, *127*, 10448−10453.
(10) (a) Olmstead, M. M.; de Bettencourt-Dias, A.; Duchamp, J. C.; Stevenson, S.; Dorn, H. C.; Balch, A. L. *J. Am. Chem. Soc.* **2000**, *122*, 12220−12226. (b) Olmstead, M. M.; de Bettencourt-Dias, A.; Duchamp, J. C.; Stevenson, S.; Marciu, D.; Dorn, H. C.; Balch, A. L *Angew. Chem., Int. Ed.* **2001**, *40*, 1223−1225.
(11) (a) Nagase, S.; Kobayashi, K.; Kato, T.; Achiba, Y. *Chem. Phys. Lett.* **1993**, *201*, 475−480. (b) Kobayashi, K.; Nagase, S. *Chem. Phys. Lett.* **1998**, *282*, 325−329. (c) Nishibori, E.; Takata, M.; Sakata, M.; Tanaka, H.; Hasegawa, M.; Shinohara, H. *Chem. Phys. Lett.* **2000**, *330*, 497−502. (d) Mizorogi, N.; Nagase, S. *Chem. Phys. Lett.* **2006**, *431*, 110−112. (e) Suzuki, M.; Lu, X.; Sato, S.; Nikawa, H.; Mizorogi, N.; Slanina, Z.; Tsuchiya, T.; Nagase, S.; Akasaka, T. *Inorg. Chem.* **2012**, *51*, 5270−5273.
(12) (a) Feng, L.; Nakahodo, T.; Wakahara, T.; Tsuchiya, T.; Maeda, Y.; Akasaka, T.; Kato, T.; Horn, E.; Yoza, K.; Mizorogi, N.; Nagase, S. *J. Am. Chem. Soc.* **2005**, *127*, 17136−17137. (b) Feng, L.; Wakahara, T.; Nakahodo, T.; Tsuchiya, T.; Piao, Q.; Maeda, Y.; Lian, Y.; Akasaka, T.; Horn, E.; Yoza, K.; Kato, T.; Mizorogi, N.; Nagase, S. *Chem.—Eur. J.* **2006**, *12*, 5578−5586. (c) Feng, L.; Tsuchiya, T.; Wakahara, T.; Nakahodo, T.; Piao, Q.; Maeda, Y.; Akasaka, T.; Kato, T.; Yoza, K.; Horn, E.; Mizorogi, N.; Nagase, S. *J. Am. Chem. Soc.* **2006**, *128*, 5990−5991.
(13) (a) Maeda, Y.; et al. *J. Am. Chem. Soc.* **2004**, *126*, 6858−6859. (b) Akasaka, T.; et al. *J. Am. Chem. Soc.* **2008**, *130*, 12840−12841. (c) Lu, X.; Nikawa, H.; Feng, L.; Tsuchiya, T.; Maeda, Y.; Akasaka, T.; Mizorogi, N.; Slanina, Z.; Nagase, S. *J. Am. Chem. Soc.* **2009**, *131*, 12066−12067. (d) Takano, Y.; Aoyagi, M.; Yamada, M.; Nikawa, H.; Slanina, Z.; Mizorogi, N.; Ishitsuka, M. O.; Tsuchiya, T.; Maeda, Y.; Akasaka, T.; Kato, T.; Nagase, S. *J. Am. Chem. Soc.* **2009**, *131*, 9340−9346.
(14) Sheldrick, G. M. *Acta Crystallogr.* **2008**, *A64*, 112−122.
(15) Frisch, M. J. et al. *Gaussian 03*, Revision C.01; Gaussian Inc.: Wallingford, CT, 2004.
(16) (a) Lee, C.; Yang, W.; Parr, R. G. *Phys. Rev. B* **1988**, *37*, 785−789. (b) Becke, A. D. *Phys. Rev. A* **1988**, *38*, 3098−3100. (c) Becke, A. D. *J. Chem. Phys.* **1993**, *98*, 5648−5652.
(17) (a) Hay, P. J.; Wadt, W. R. *J. Chem. Phys.* **1985**, *82*, 299−310. (b) Francl, M. M.; Pietro, W. J.; Hehre, W. J.; Binkley, J. S.; Gordon, M. S.; DeFrees, D. J.; Pople, J. A. *J. Chem. Phys.* **1982**, *77*, 3654−3665.
(18) Haddon, R. C. *Science* **1993**, *261*, 1545−1550.